JOURNAL OF VIROLOGY, Mar. 2009, p. 2327–2337 Vol. 83, No. 5
0022-538X/09/$08.00+0 doi:10.1128/JVI.02184-08

Vacuolar Protein Sorting Pathway Contributes to the Release of Marburg Virus▽

Larissa Kolesnikova,[1,3]† Thomas Strecker,[1]† Eiji Morita,[4] Florian Zielecki,[1,3] Eva Mittler,[1] Colin Crump,[2] and Stephan Becker[1,3]*

Institut für Virologie, Philipps-Universität Marburg, Hans-Meerwein-Str. 2, 35043 Marburg,[1] and Robert Koch-Institut, Berlin, Nordufer 20, 13353 Berlin,[3] Germany; Department of Pathology, University of Cambridge, Tennis Court Road, CB2 1QP Cambridge, United Kingdom[2]; and University of Utah School of Medicine, Salt Lake City, Utah 84132[4]

Received 16 October 2008/Accepted 2 December 2008

VP40, the major matrix protein of Marburg virus, is the main driving force for viral budding. Additionally, cellular factors are likely to play an important role in the release of progeny virus. In the present study, we characterized the influence of the vacuolar protein sorting (VPS) pathway on the release of virus-like particles (VLPs), which are induced by Marburg virus VP40. In the supernatants of HEK 293 cells expressing VP40, different populations of VLPs with either a vesicular or a filamentous morphology were detected. While the filaments were almost completely composed of VP40, the vesicular particles additionally contained considerable amounts of cellular proteins. In contrast to that in the vesicles, the VP40 in the filaments was regularly organized, probably inducing the elimination of cellular proteins from the released VLPs. Vesicular particles were observed in the supernatants of cells even in the absence of VP40. Mutation of the late-domain motif in VP40 resulted in reduced release of filamentous particles, and likewise, inhibition of the VPS pathway by expression of a dominant-negative (DN) form of VPS4 inhibited the release of filamentous particles. In contrast, the release of vesicular particles did not respond significantly to the expression of DN VPS4. Like the budding of VLPs, the budding of Marburg virus particles was partially inhibited by the expression of DN VPS4. While the release of VLPs from VP40-expressing cells is a valuable tool with which to investigate the budding of Marburg virus particles, it is important to separate filamentous VLPs from vesicular particles, which contain many cellular proteins and use a different budding mechanism.

In recent years, virus-like particles (VLPs), which are formed upon recombinant expression of the viral matrix and/or surface glycoproteins, have been recognized as representing powerful tools for developing novel vaccines and investigating certain aspects of the viral replication cycle (24, 44, 59, 63). Matrix proteins from many enveloped RNA viruses, including retroviruses, rhabdoviruses, filoviruses, paramyxoviruses, orthomyxoviruses, and arenaviruses, are able to induce VLPs (10, 14, 18, 28–30, 48, 49, 52). Increasing evidence also indicates that budding activity, and thus the release of VLPs, is often influenced by a complex interplay with components of the endosomal sorting complexes required for transport (ESCRTs), which mainly constitute the vacuolar protein sorting (VPS) pathway (16, 38, 42, 54). ESCRTs trigger the formation and budding of vesicles into the lumina of multivesicular bodies (MVBs), and the constituents of the ESCRTs are recycled by the activity of VPS4, an AAA-type ATPase. Expression of dominant-negative (DN) VPS4 mutants, which lack the ability to bind or hydrolyze ATP, blocks recycling of the ESCRTs and induces the formation of enlarged endosomes lacking internal vesicle accumulation (2, 3, 7). The inward budding of vesicles into the MVBs is topologically similar to the budding of viruses, since the vesicles bud away from the cytosol and into the lumen (reviewed in references 1, 20, and 26). Therefore, it is not entirely surprising that viruses use the cellular ESCRT machinery to organize the budding of viral progeny. Interactions between viral matrix proteins and ESCRTs occur through tetrapeptide motifs, known as late domains, which were first identified in retroviruses. Known late domains consist of the amino acid sequence P(T/S)AP, PPxY, or YxxL, where "x" represents any amino acid (19, 25, 62). The P(T/S)AP motif, for example, mediates interaction with tumor susceptibility gene 101 (Tsg101) (16, 36, 57); the PPxY motif mediates binding to WW domains of Nedd4-like ubiquitin ligases (9, 22); and the YxxL motif mediates interaction with AIP1/Alix (35, 47, 58). Recently, a novel late-domain motif, FPIV, has been identified in paramyxoviruses (46), and it is thought that additional late-domain motifs remain to be discovered (for a review, see reference 5).

Inhibition of the VPS pathway has been shown to inhibit the budding of various viruses that are released with the help of ESCRTs. However, the budding of viruses and VLPs depends on the activity of ESCRTs to different degrees. Downregulation of Tsg101, a member of the ESCRT-I complex, inhibited the release of VLPs mediated by lymphocytic choriomeningitis virus Z protein and Marburg virus (MARV) VP40 (42, 54) but did not substantially inhibit the release of Gag-induced VLPs of Moloney murine leukemia virus and Rous sarcoma virus or that of matrix protein-induced VLPs of rabies virus (16, 27, 38). Expression of DN VPS4 inhibited the release of VLPs induced by the Gag proteins of Rous sarcoma virus and Moloney murine leukemia virus (16, 38) as well as that of VLPs induced by Lassa virus Z protein (55) but had no effect on the

* Corresponding author. Mailing address: Institut für Virologie, Philipps-Universität Marburg, Hans-Meerwein-Str. 2, Marburg D-35043, Germany. Phone: 49-06421-2866253. Fax: 49-06421-2868962. E-mail: becker@staff.uni-marburg.de.

† L.K. and T.S. contributed equally to this work.

▽ Published ahead of print on 17 December 2008.

budding of rabies virus and cytomegalovirus (13, 27). These data indicate that in spite of the presence of late-domain motifs, a block in the VPS pathway may not always be critical for the budding of VLPs. In addition, the lack of known late domains in many enveloped viruses raises the question of whether they use other entry points into the VPS pathway or whether they exploit entirely different mechanisms of budding (60). To date, knowledge of how viral matrix proteins engage cellular machineries, such as the VPS pathway, to induce viral budding at the plasma membrane is very limited (8).

The matrix protein VP40 of MARV contains only one known late-domain motif, PPPY, and a recent study showed that mutation of this late domain inhibited the release of VP40-induced VLPs. In addition, depletion of Tsg101 reduced the release of VP40-induced VLPs, suggesting that ESCRT-I is involved in this process (54). Whether a functional VPS pathway is important for the release of MARV VP40-induced VLPs or MARV particles remains unknown.

VLPs induced by many viral matrix proteins have a morphology similar to that of cellular vesicles, which makes it difficult to separate the spherical VLPs from released cellular vesicles (4, 17, 53). In contrast, VLPs induced by the filovirus matrix protein VP40 are elongated and similar in morphology to viral particles (30, 49). Nevertheless, we observed that the supernatants of cells expressing VP40 contained various populations of particles with different morphologies. This raised the questions of whether the different particles are released by the same mechanism, whether they are all induced by VP40, and whether they are dependent on the same cellular pathways.

The aim of the present study was to analyze the populations of particles released from cells expressing the MARV matrix protein VP40 and to gain further insights into the interaction between MARV and the cellular machinery involved in the budding of VLPs and MARV particles.

We found that cells expressing VP40 released vesicular and filamentous particles, which could be separated by gradient centrifugation. Fractions with mainly vesicular particles represented a mixture of vesicles containing exclusively cellular proteins and vesicles also containing VP40 and few short filamentous particles. Longer filamentous particles, whose morphology resembled that of MARV particles but which displayed a much higher variability in length (400 nm to 5 μm), were found in denser gradient fractions. Filamentous VP40-induced VLPs were able to sort out cellular proteins efficiently. Release of VP40-induced filamentous VLPs was supported by the late-domain motif present in VP40, and inhibition of the cellular ESCRT machinery reduced the amount of these VLPs in the supernatant. Interestingly, the release of VLPs induced by a mutant of VP40 lacking the late domain was also reduced by inhibition of the cellular ESCRT machinery. Expression of a DN mutant of VPS4 diminished the budding of infectious MARV particles by 50%, a finding consistent with the idea that the activity of the ESCRT machinery supports viral budding but is not essential.

MATERIALS AND METHODS

Cell lines. Human embryonic kidney cells (HEK 293) and human hepatoma cells (HUH-7) were maintained in Dulbecco's modified Eagle medium supplemented with 10% fetal calf serum, L-glutamine, and penicillin-streptomycin solution. An inducible human embryonic kidney (iHEK 293) cell line expressing enhanced green fluorescent protein (EGFP)-tagged human VPS4 with the active-site glutamate (position 228) changed to glutamine (E228Q) (11) (EGFP-VPS4-E228Q) was also used. Transcription of the EGFP-VPS4-E228Q gene was under the control of an ecdysone-responsive element; thus, ponasterone A (Invitrogen) was required to stimulate gene expression. iHEK 293 cells were propagated in Dulbecco's modified Eagle medium supplemented with 200 μg/ml Zeocin and 400 μg/ml G418 for long-term maintenance of EGFP-VPS4-E228Q gene expression. The cells were grown at 37°C under 5% CO_2. HUH-7 cells were used for immunofluorescence analysis, while HEK 293 cells were used for the investigation of VLP release.

Molecular cloning and plasmids. For the mutation of the PPPY late-domain motif in MARV VP40, the tyrosine residue at position 19 was replaced with an alanine by using the QuikChange site-directed mutagenesis kit (Stratagene) with pC-VP40 as a template (40). The resulting vector was designated pC-$VP40_{PPxA}$. Insertion of the Ebola virus (EBOV) overlapping late-domain motifs (PTAPPEY) instead of the single MARV late-domain motif (PPPY) was performed by PCR amplification using two 5′-phosphorylated primers containing the coding sequence for the overlapping late-domain motifs of EBOV (40). A plasmid encoding a fusion protein consisting of the *Aequorea coerulescens* green fluorescent protein (GFP) and the N-terminal membrane-targeting signal of neuromodulin (GFP-mem) was obtained from Clontech Laboratories. A plasmid encoding the human Tsg101 gene was a gift from Paul D. Bieniasz (New York, NY). A Flag tag was introduced into this construct at the N terminus by standard PCR, and the tagged construct was cloned via NheI and HindIII into the pCAGGS vector by Robert Eichler (Institute of Virology, Philipps University Marburg). All constructs were verified by DNA sequencing.

Antibodies. For the identification of MARV VP40, a mouse monoclonal antibody (kindly provided by M. C. Georges-Courbot, France) and a goat polyclonal antibody were used for immunofluorescence analysis (dilutions, 1:50 and 1:100, respectively) and for Western blot analysis (dilutions, 1:1,000 and 1:3,000, respectively). A goat anti-GFP polyclonal antibody (dilution, 1:1,000) was used for the detection of GFP and GFP fusion proteins in Western blot analysis (Rockland). Secondary antibodies conjugated to horseradish peroxidase (Dako) were used with Alexa Fluor R680 or with IRDye 800 (Rockland) for Western blot analysis (dilution, 1:5,000). Secondary antibodies conjugated to rhodamine or fluorescein isothiocyanate (Dianova) were used for immunofluorescence analysis at a dilution of 1:200.

Transfection of cells. HEK 293 or HUH-7 cells were transfected using the FuGENE 6 transfection reagent (Roche) according to the manufacturer's instructions. Transfected cells were incubated at 37°C under 5% CO_2 for 24 h.

Purification of vesicular and filamentous particles extracted from cellular supernatants. At 24 h posttransfection, cellular supernatants from HEK 293 cells were harvested, and vesicular and filamentous particles were purified as described previously (31, 39). Briefly, the supernatants were pelleted in an SW41 rotor (Beckman) through a 20% sucrose cushion at 35,000 rpm for 3 h at 4°C. The pellet was resuspended in TNE buffer (10 mM Tris-HCl [pH 7.5], 150 mM NaCl, 1 mM EDTA [pH 8]), laid on a Nycodenz (Axis-Shield) step gradient, and centrifuged in an SW60 rotor at 16,000 rpm for 15 min at 4°C. The Nycodenz gradient was composed of seven steps containing 2.5% to 30% Nycodenz from the top to the bottom. Fractions (500 μl) were collected from the top, and as indicated, fractions 1 to 3 (vesicular particles) and fractions 4 to 6 (filamentous particles) were pooled. To concentrate membranes and membrane-associated proteins, pooled fractions were centrifuged in a TLA45 rotor (Beckmann) at 45,000 rpm for 2 h at 4°C. The resultant pellets were resuspended in equal amounts of buffer and subjected to either sodium dodecyl sulfate-polyacrylamide gel electrophoresis and Coomassie staining, Western blot analysis, or electron microscopic analysis. In any case, equal volumes of resuspended pellets were analyzed in order to compare fractions 1 to 3 with fractions 4 to 6.

Electrophoresis and immunoblot analysis. Western blot analysis was carried out as described previously (30). The antibodies are listed in the figure legends. The intensities of the bands for cell- and VLP-associated proteins were quantified using the Odyssey imaging system (Licor).

Indirect immunofluorescence analysis. At 24 h posttransfection, HUH-7 cells were washed with phosphate-buffered saline (PBS) and fixed with 4% paraformaldehyde for 30 min. The fixative was removed, and free aldehydes were quenched with 100 mM glycine in PBS. Afterwards, the samples were washed once with PBS and permeabilized with 0.1% Triton X-100 in PBS. Cells were incubated in blocking solution (2% bovine serum albumin, 0.2% Tween 20, 5% glycerol, and 0.05% sodium azide in PBS) and stained with primary and secondary antibodies as indicated below (see the figure legends). Microscopic analysis was performed with a fluorescence microscope (Axiomat; Zeiss).

Yeast two-hybrid binding assays. Directed yeast two-hybrid assays were performed as described previously (33, 58). Briefly, *Saccharomyces cerevisiae* AH-109 was cotransformed with the pGADT7 and pGBKT7 cloning vectors (Clontech) containing the inserts of interest. The transformed yeast colonies were grown for 3 days at 30°C on yeast extract-peptone-dextrose plates without Leu and Trp for selection. Ten to 100 colonies were pooled, resuspended in a liquid culture of Sabourand dextrose broth (without Leu and Trp), selected on Sabourand dextrose broth (without Leu, Trp, Ade, and His) plates for growth of $Leu^+Trp^+Ade^+His^+$ colonies, and allowed to grow for 3 days.

Viral replication assays. The infectivities of MARV (Musoke) or EBOV (Zaire) particles released into the supernatants of cells expressing a DN VPS4 were assayed by a 50% tissue culture infective dose ($TCID_{50}$) assay and an immunofluorescence focus-forming (IFF) assay. For the $TCID_{50}$ assay, Vero cells were grown in 96-well plates to 30 to 40% confluence. Cells were inoculated with 10-fold serial dilutions of supernatants of filovirus-infected iHEK 293 cells grown in the presence or absence of ponasterone A. The assay results were evaluated at 10 to 12 days postinfection. $TCID_{50}$s were calculated using the Spearman-Karber method (23). For the IFF assay, Vero cells were grown on coverslips in 24-well plates to 50% confluence. Cells were inoculated with 10-fold serial dilutions of supernatants of filovirus-infected iHEK 293 cells grown in the presence or absence of ponasterone A. Cells were fixed at 1 day postinfection and immunostained with a mouse monoclonal antibody against NP; then NP-positive cells were counted. All experiments involving MARV- and EBOV-infected samples were performed under biological safety level 4 conditions at the Philipps-University Marburg.

RESULTS

Particles in the supernatants of VP40-expressing cells represent a mixture of filamentous and vesicular forms. Particles derived from cells expressing MARV VP40 are heterogeneous in terms of length and shape (30, 49, 59). In order to better understand the nature of the different particles, we screened particulate material released into the supernatants of cells expressing VP40. Supernatants were concentrated by centrifugation through a sucrose cushion, and pellets were separated by density gradient centrifugation and subsequent fractionation. Particulate material was pelleted from the resulting fractions, and pellets were subjected to immunoelectron microscopic analysis using VP40-specific antibodies (Fig. 1A and B). Fractions 1 to 3 contained (i) small round vesicles exclusively made of cellular proteins, (ii) small round vesicles positive for VP40, and (iii) short or ring-like forms of filamentous VLPs (Fig. 1A). Fractions 4 to 6 contained only filamentous particles of different lengths; some exceeded several micrometers (Fig. 1B, top). More than 95% of filamentous VLPs were strongly positive for VP40, as indicated by immunogold labeling (Fig. 1B, top) and displayed a regular striation in negative staining, which was also detected in viral particles (32) (Fig. 1B, bottom). Similar striation was observed in the short forms of filamentous VLPs detected in vesicular fractions 1 to 3 (Fig. 1C). To understand the contribution of VP40 to the formation of the released particles, supernatants from cells expressing a membrane-associated GFP-tagged peptide corresponding to the N-terminal 20 amino acids of neuromodulin (GFP-mem) were analyzed. The neuromodulin fragment contains a signal for posttranslational palmitoylation of cysteines at positions 3 and 4, which targets the fusion protein to cellular membranes, the plasma membrane in particular. In contrast to VP40, GFP-mem does not contain any known late-domain motif. The vast majority of particles in the supernatants of cells expressing GFP-mem were spherical vesicles, which were partly positive for GFP (Fig. 1D, left). Very rarely, slightly elongated vesicles (approximately 400 nm long) whose appearance differed completely from that of the filaments observed in the supernatants of VP40-expressing cells were detected in fractions 4 to 6 (Fig. 1D, right). These findings indicate that expression of VP40 specifically induced the formation of filamentous VLPs displaying regular striation. Possibly, vesicles and filaments are subjected to different release strategies.

Regular arrangement of VP40 in filamentous particles excludes cellular proteins. Published data have shown that several cell types, especially tumor cells, release membrane vesicles with diameters of 30 to 100 nm into the cell culture supernatant (for a review, see reference 56). These vesicles represent a mixture of exosomes, which are released into the extracellular milieu after the fusion of MVBs with the plasma membrane, and plasma membrane-limited vesicles, which are shed due to the dynamic nature of the cell surface (21, 43). It has been shown that exosomes contain cytoskeletal proteins (e.g., actin, tubulin, and moesin), ESCRT proteins (Tsg101, Alix), integrins, and proteins involved in the transport and fusion of intracellular vesicles (reviewed in references 12 and 51).

Since we have found that supernatants of VP40-expressing cells represent a mixture of filaments and vesicles, it was of interest to screen the different particles for their cellular-protein contents. Coomassie blue staining of gradient-purified particles showed that particles from the filamentous fractions consist predominantly of VP40 (Fig. 2A, lane 2) while particles from the vesicular fractions contain mainly cellular proteins (Fig. 2A, lane 1). Immunoblot analysis clearly identified α-tubulin, actin, and Tsg101 in vesicular fractions derived from cells expressingVP40, GFP-mem, or GFP and in vesicles derived from mock-transfected cells (Fig. 2B, top, lanes 1, 3, 5, and 7). In contrast, filamentous VLPs contained much less cellular protein. In fact, neither α-tubulin nor actin nor Tsg101 was detected in filamentous VLPs at 24 h after transfection, indicating that these VLPs, like virions, were able to efficiently exclude cellular proteins during formation and budding (Fig. 2B, top, lanes 2, 4, 6, and 8). These data indicate that particulate material in the supernatants of VP40-expressing cells contains large amounts of vesicles that are not specifically induced by VP40. Moreover, the data suggested that only the filamentous particles can be considered authentic VP40-induced VLPs whose formation and release might reflect the budding of MARV.

VP40 late domain influences VLP release. Next, we wanted to determine how the late-domain motif of VP40 ($P_{16}PPY_{19}$) influenced the release of particles from VP40-expressing cells. Therefore, we constructed two mutants of VP40 in which either the tyrosine residue at position 19 was replaced by alanine ($VP40_{PPxA}$) or the late-domain motif was replaced by the two overlapping late domains of EBOV VP40 ($VP40_{ELD}$). To test whether the inserted EBOV late-domain motif was functional, we coexpressed $VP40_{ELD}$ with Tsg101. Immunofluorescence analysis showed that in contrast to MARV VP40 and $VP40_{PPxA}$, $VP40_{ELD}$ induced redistribution of Tsg101 into peripheral VP40-positive clusters (Fig. 3A). This result was expected, because redistribution of Tsg101 to the plasma membrane has been observed for EBOV VP40 (36). Thus, we concluded that $VP40_{ELD}$, due to its interaction with Tsg101, contained an additional entry site to the ESCRT machinery, which might be beneficial for budding.

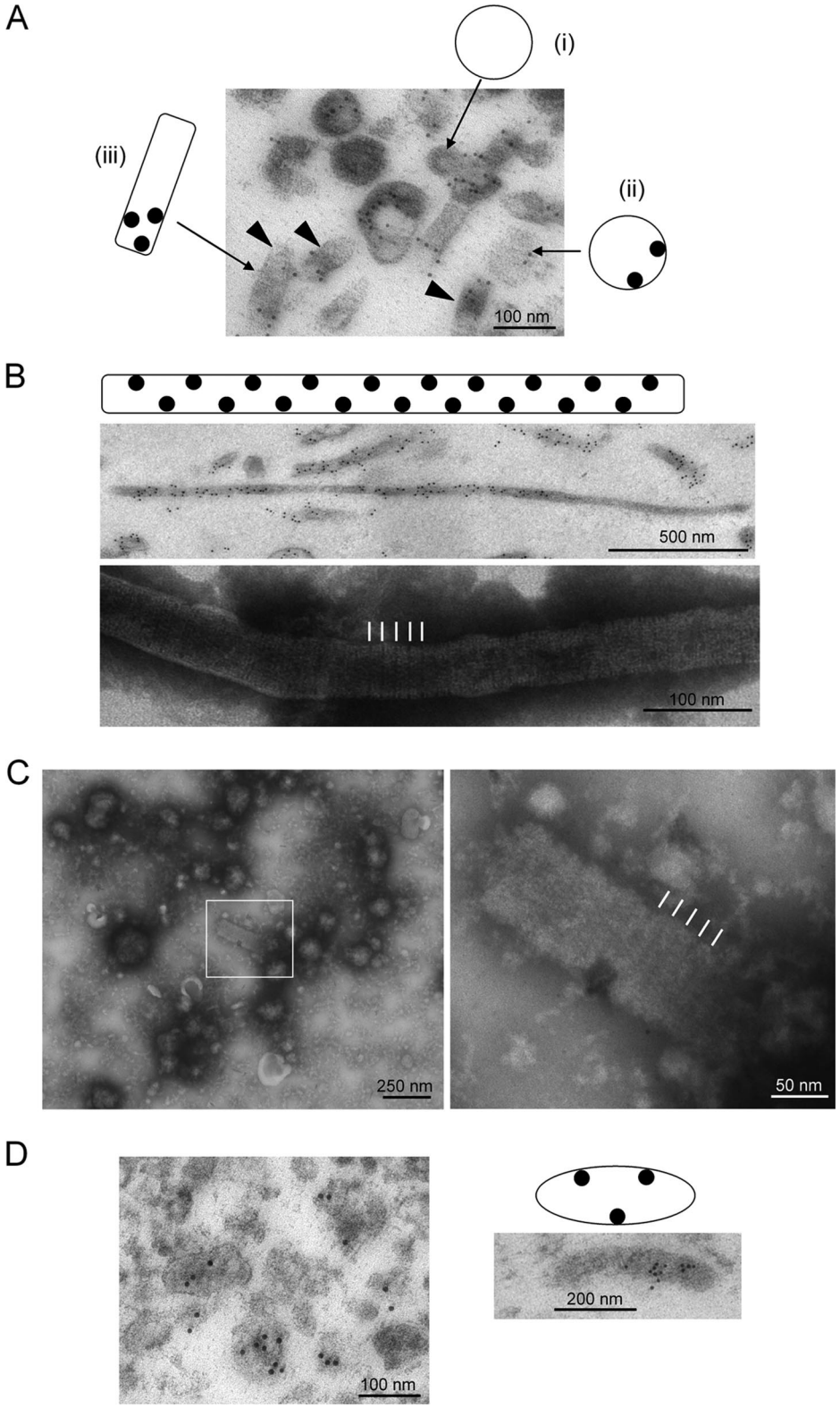

FIG. 1. Immunoelectron microscopic analysis of VP40- and GFP-mem-induced VLPs. VLPs were purified from the supernatants of HEK 293 cells expressing either VP40 or GFP-mem. Fractions containing vesicular or filamentous VLPs were fixed in 4% paraformaldehyde, dehydrated, and embedded in LR White. (A to C) VP40-induced VLPs. (A) Fractions 1 to 3 (vesicular fractions). (i) Small round vesicles containing cellular proteins only; (ii) small round vesicles positive for VP40; (iii) short or ring-like filamentous VLPs (arrowheads). Ultrathin sections were immunostained with a mouse monoclonal antibody against VP40 (5-nm-diameter gold particles). (B) Fractions 4 to 6 (filamentous fractions). (Top) Immunostaining with a VP40-specific mouse monoclonal antibody; (bottom) negative staining. (C) (Left) Negatively stained vesicular fractions; (right) enlarged image of a short filamentous particle. (D) GFP-mem-induced VLPs. Ultrathin sections were immunostained with a goat polyclonal antibody against GFP (10-nm-diameter gold particles). (Left) Spherical vesicles; (right) slightly elongated vesicles. Schematic drawings (A, B, and D) illustrate forms of particles and the presence of colloidal gold.

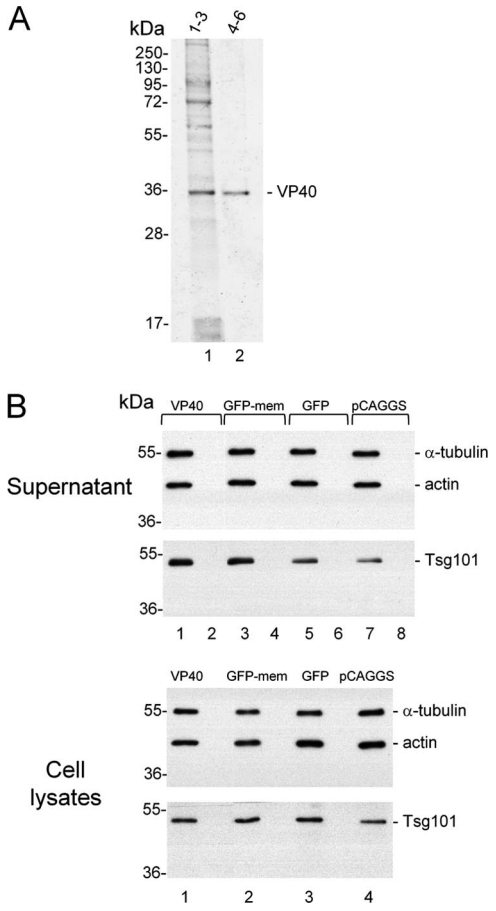

FIG. 2. Detection of cellular proteins in vesicular and filamentous VLPs induced by wild-type VP40, GFP-mem, or GFP. HEK 293 cells were transfected with a plasmid encoding either wild-type VP40, GFP-mem, or GFP, or with the empty pCAGGS vector. (A) Coomassie blue staining of vesicular (fractions 1 to 3) (lane 1) and filamentous (fractions 4 to 6) (lane 2) fractions of VLPs induced by wild-type VP40 expression. (B) Cellular lysates (bottom) and VLPs (top [odd-numbered lanes, vesicular particles; even-numbered lanes, filamentous particles]) were subjected to Western blot analysis to detect cellular proteins (actin, α-tubulin, and Tsg101).

Cells were transfected with plasmids encoding VP40, $VP40_{PPxA}$, $VP40_{ELD}$, GFP-mem, or GFP. All recombinant proteins were detected in the cell lysates (Fig. 3B, top), and all, except for GFP, were released into the culture supernatant in association with particulate material (Fig. 3B, bottom, lanes 1 to 10). Quantification of Western blots showed that the relative levels of VP40 in fractions containing mainly vesicular or filamentous particles were 70% and 29%, respectively (Fig. 3C). The levels of released particulate VP40 dropped to 42% and 14%, respectively, when the late domain of VP40 was disrupted (Fig. 3C, $VP40_{PPxA}$). Interestingly, insertion of the overlapping late-domain motifs of EBOV VP40 enhanced the release of MARV $VP40_{ELD}$, mainly in the fractions containing vesicles (140%), while the release of $VP40_{ELD}$ in the fraction containing filaments remained constant (31%) (Fig. 3C). We then determined the number of short filamentous particles in the vesicular fractions by electron microscopy. This analysis showed that the frequency of short filamentous particles dropped from 52 to 30 per 1,000 vesicles when the late domain of VP40 was destroyed (58% of the number for wild-type VP40 [Fig. 3D]). This result suggested that the decreased release of VP40-positive particles in the vesicular fractions is attributable mainly to decreased filamentous-particle production. When the ELD construct was inserted into MARV VP40, the number of short filamentous particles increased from 52 to 95 per 1,000 vesicular particles (183% of the number for wild-type VP40), again paralleling the results of Western blot analysis (compare Fig. 3B, bottom, and D). It is presumed that the presence of the ELD construct favored the formation of short filamentous particles, while the formation and release of longer filaments, represented by the VP40 signal in gradient fractions 4 to 6, remained constant (Fig. 3B, bottom, lanes 2 and 6). GFP-mem was detected almost exclusively in the vesicular fractions (Fig. 3B, bottom, lanes 7 and 8).

Taken together, the data presented showed that the release of short and long VP40-containing filamentous particles is sensitive to the presence of late domains. Since the short filamentous particles in fractions 1 to 3 were contaminated by vesicles that did not respond to changes in the late domain of VP40, we decided to focus further analyses on the pure filamentous particles obtained from fractions 4 to 6 of the gradient.

Influence of a DN mutant of VPS4 on the release of VP40-induced VLPs. The budding of retroviruses possessing any of the three major types of late-domain motifs is inhibited by DN AAA-type ATPase VPS4 (16, 37). To test if the budding of MARV VP40-induced VLPs is also dependent on the VPS pathway, we expressed VP40 and mutants of VP40 in a HEK 293 cell line that inducibly expressed DN VPS4 (VPS4-E228Q) fused to EGFP (11). Almost identical amounts of VP40 and mutants of VP40 were detected, indicating that expression levels were not significantly influenced by the presence of DN VPS4 (Fig. 4A). By immunofluorescence analysis we have found that both wild-type VPS4 (VPS4-wt) and DN VPS4 were partially recruited into the peripheral VP40-positive clusters. The intracellular distribution patterns of VP40 and mutants of VP40 were similar in the presence of DN VPS4 or VPS4-wt (data not shown). Western blot analyses of the respective supernatants revealed that DN VPS4 reduced the release of VP40-, $VP40_{PPxA}$-, and $VP40_{ELD}$-induced filamentous particles to 46%, 17%, and 39%, respectively (Fig. 4B and F). Notably, expression of VPS4-wt fused to EGFP (EGFP-VPS4-wt) did not influence the release of VLPs induced by VP40 and mutants of VP40 (Fig. 4C and D). GFP-mem could be observed only in association with vesicles in fractions 1 to 3, whose release was not influenced by the expression of DN VPS4 (Fig. 4E). Moreover, vesicles containing GFP-mem also contained EGFP-VPS4-E228Q, which was not detectable in the filamentous VP40-induced particles (Fig. 4B and E). These data indicate that (i) release of VP40-induced VLPs is partly dependent on the VPS pathway; (ii) release of $VP40_{PPxA}$-containing VLPs was also influenced by the presence of EGFP-VPS4-E228Q, suggesting that MARV VP40 contains additional means to interact with ESCRTs besides binding to Nedd4-like ubiquitin ligases; and (iii) GFP-mem-containing cellular vesicles released in the absence of the viral matrix protein were not influenced by the

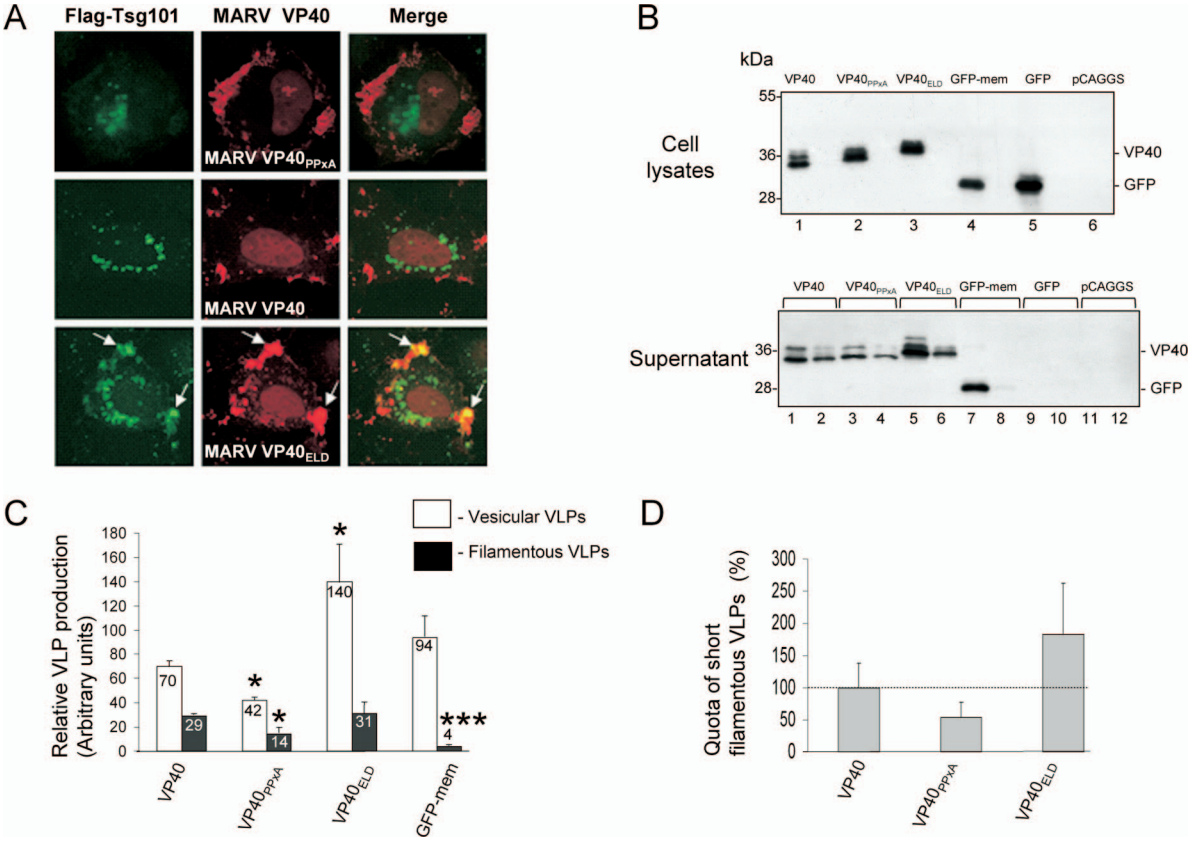

FIG. 3. Characterization of proteins and purification of vesicular and filamentous VLPs. (A) Immunofluorescence analysis of VP40 mutants. HUH-7 cells were transfected with a plasmid encoding wild-type VP40, or VP40 mutants, and with Flag-tagged Tsg101. Cells were fixed at 24 h posttransfection and immunostained with a rabbit anti-Flag and a mouse anti-VP40 antibody. Bound antibodies were detected using goat anti-rabbit immunoglobulin G coupled with fluorescein isothiocyanate and goat anti-mouse immunoglobulin G conjugated with rhodamine as secondary antibodies. The arrows indicate colocalization of $VP40_{ELD}$ and Tsg101. (B) Western blot analysis of the production of vesicular and filamentous VLPs induced by wild-type VP40, VP40 mutants, GFP-mem, or cytosolic GFP. HEK 293 cells were transfected either with a plasmid encoding either wild-type VP40, a VP40 mutant, GFP-mem, or GFP or with the control vector. Cell lysates (top) and VLPs (bottom [odd-numbered lanes, vesicular particles; even-numbered lanes, filamentous particles]) were collected at 1 day posttransfection, and Western blot analysis was performed to detect VP40 and GFP. (C) The intensities of the bands for cell- and VLP-associated VP40, GFP-mem, and GFP in panel B were quantified using the Odyssey imaging system. The budding efficiency of VLPs induced by wild-type VP40 (VLP-associated VP40/cell-associated VP40) was set at 100. Data are averages, with standard deviations, from at least three independent experiments. Asterisks indicate statistically significant differences (*, $P < 0.05$; **, $P < 0.01$; ***, $P < 0.001$). (D) Relative frequencies of short filamentous particles in the fractions of vesicular VLPs. Quantification was done on random electron micrograph images of negatively stained samples. The quota of short filamentous particles (number per 1,000 vesicles) induced by wild-type VP40 was set at 100% (dashed horizontal line).

ESCRT machinery, suggesting that these vesicles use different budding factors.

MARV VP40 interacts with ubiquitin-like ligases. To determine whether VP40 was able to interact with other ESCRT proteins besides Nedd4-like ubiquitin ligases, we tested interactions between MARV VP40 and all known human class E proteins using yeast two-hybrid assays (58). As a control, we also tested EBOV VP40. As expected, EBOV VP40 interacted with Tsg101 and NEDL1, while MARV VP40 showed interaction only with AIP2, AIP4, and AIP5 (Fig. 5). Two-hybrid analyses were possible only in one direction, because the GAL4 DNA binding domain fused to MARV VP40 (DBD-MARV-VP40) was self-activating in yeast two-hybrid vectors (data not shown). In addition, both, MARV and EBOV VP40 proteins gave positive signals for LIP5. However, the significance of this result is not clear, because DBD-Lip5 shows positive interaction with most proteins that have been tested. The results of the two-hybrid screen suggested that no unexpected interactions between ESCRT proteins and MARV VP40 take place, leaving the impact of the ESCRT machinery on the release of $VP40_{PPxA}$ enigmatic.

Budding of MARV is inhibited in a stable cell line inducibly expressing DN VPS4. It has been shown previously that release of infectious EBOV particles was diminished 10-fold in the presence of DN VPS4 (34). However, it is not clear whether a functional VPS pathway is important for MARV budding. To address this question, we infected iHEK 293 cells with MARV or EBOV in the presence of ponasterone A to induce the expression of VPS4-wt or DN VPS4. Cell lysates and supernatants were harvested at 24 h postinfection, and Western blot analysis was performed (Fig. 6A and B). While expression of DN VPS4 did not change the intracellular amounts of NP and VP40, the release of these viral proteins was reduced by approximately 50% for both MARV and EBOV (Fig. 6A and B,

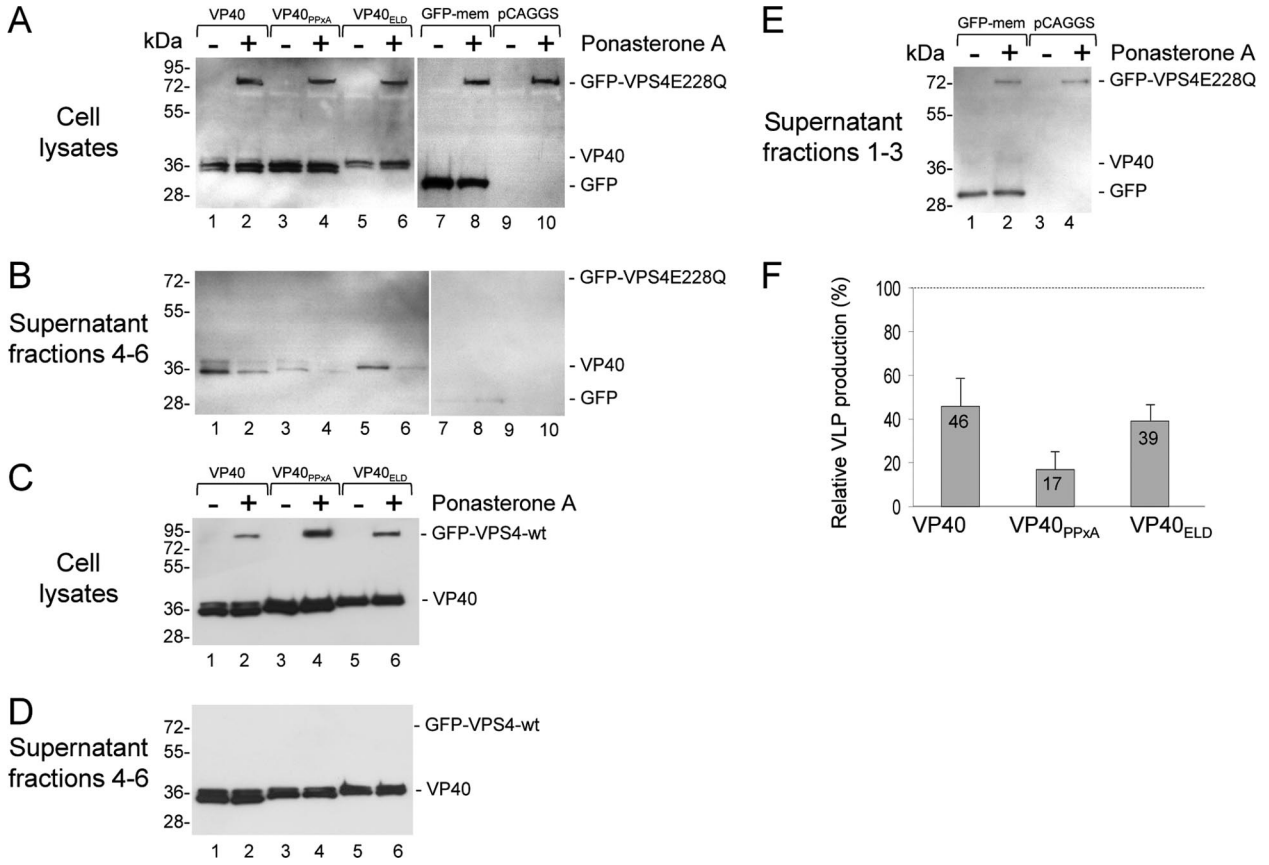

FIG. 4. Effect of DN VPS4 on the release of vesicular and filamentous VLPs. (A and B) An inducible (iHEK 293) cell line expressing EGFP-VPS4-E228Q under the control of an ecdysone-responsive element was transfected with a plasmid encoding either wild-type VP40, VP40 mutants or GFP-mem. Expression of EGFP-VPS4-E228Q either was not induced (−) or was induced (+) with 1 μM ponasterone A at the time of transfection. (A) Cell lysates; (B) filamentous VLPs. (C and D) As a control, an inducible (iHEK 293) cell line expressing EGFP-VPS4-wt was transfected with a plasmid encoding either wild-type VP40 or VP40 mutants. Expression of EGFP-VPS4-wt either was not induced (−) or was induced (+) at the time of transfection with 1 μM ponasterone A. (C) Cell lysates; (D) filamentous VLPs. (E) Vesicular VLPs purified from EGFP-VPS4-E228Q-expressing cells transfected with a GFP fusion protein or an empty vector. Expression of EGFP-VPS4-E228Q either was not induced (−) or was induced (+) with 1 μM ponasterone A at the time of transfection. (F) The intensities of the bands for cell- and VLP-associated VP40 in panels A and B were quantified using the Odyssey imaging system. The budding efficiency of VLPs induced by the proteins analyzed in iHEK 293 cells not expressing EGFP-VPS4-E228Q was set at 100% (dashed horizontal line). Data are averages and standard deviations from at least three independent experiments.

lanes 10, and C). To determine whether virions released into the supernatant were infectious, clarified culture supernatants from infected cells were used to infect Vero cells, which were fixed and analyzed by an IFF assay at 24 h postinfection (Fig. 6D). Expression of DN VPS4 significantly diminished the release of infectious EBOV (approximately 11-fold) and MARV (approximately 3-fold) (Fig. 6D) particles. Similar effects were observed in a $TCID_{50}$ assay carried out at 48 h postinfection (Table 1).

Taken together, the data show that VP40 specifically induced the release of filamentous VLPs, which were similar in morphology to MARV particles. VP40 in these filamentous VLPs was organized in a regular array beneath the lipid envelope and was able to sort out cellular proteins efficiently. Additionally, VP40-expressing cells secreted a mixture of VP40-positive and VP40-negative vesicles that contained several cellular proteins. While the release of filamentous VLPs was partly dependent on the activity of the ESCRT machinery, the release of vesicles was not. In line with this result, the release of filamentous VLPs was partly dependent on the activity of the single late domain in VP40. However, even in the absence of the late domain, the budding of filamentous VLPs was influenced by the VPS pathway. Finally, the release of MARV particles was dependent on the ESCRT machinery, like that of VP40-induced filamentous VLPs.

DISCUSSION

Release of filamentous MARV VP40-induced VLPs is sensitive to VPS pathway function. The filoviral matrix protein VP40 was shown to induce the formation of VLPs that were similar in shape and size to the respective filoviral particles (49, 52). Preparations obtained from supernatants of VP40-expressing cells, however, also contained vesicular particles of unknown origin that were released from control cells. It was therefore of interest to analyze the nature of the different enveloped particles and their respective release into the supernatant. We developed a method to separate the released par-

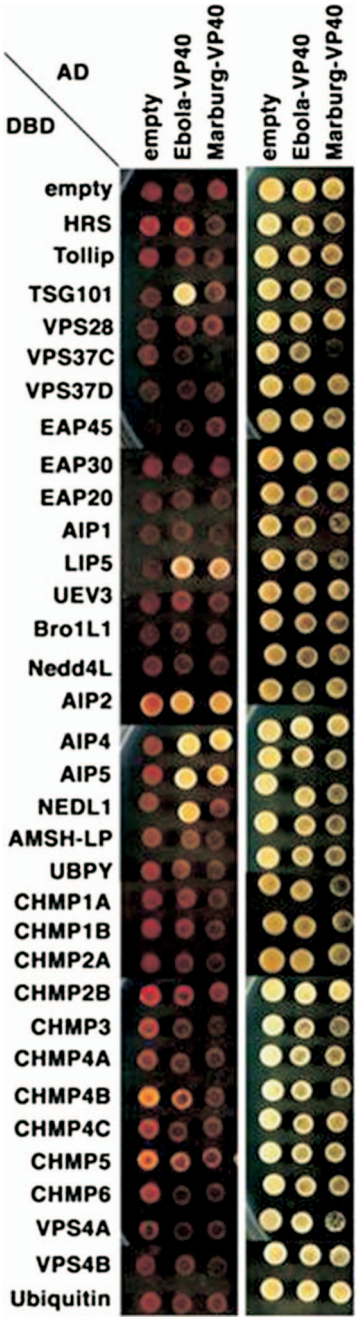

FIG. 5. Yeast two-hybrid interactions between MARV VP40, EBOV VP40, and all known human class E proteins. The indicated constructs were fused to the DBD or activation domain (AD), coexpressed, and tested for positive yeast two-hybrid interactions (left column) (medium without Trp, Leu, His, and Ade) or cotransformation (control) (right column) (medium without Trp and Leu). Unfused DBD and AD constructs are shown as negative controls.

ticles based on their densities into two fractions, which contained either mainly vesicular or filamentous VLPs (39). In the present study, we found that the vesicular fraction also included a small number of short VP40-induced filamentous particles, while the filamentous fraction was pure. The filamentous VLPs consisted mainly of VP40, which was arranged in a regular array beneath the envelope, while the vesicular particles contained many cellular proteins. This result indicated that the filoviral matrix protein VP40 is able to exclude cellular proteins from the developing filamentous viral particles. A similar role for a matrix protein has been described for the influenza virus M1 protein (41). The finding that differentiation between released vesicles and filamentous VLPs is possible makes the MARV VLPs especially attractive as a tool with which to investigate viral budding. The spherical nature of many other viruses, e.g., human immunodeficiency virus type 1 and influenza virus, and their related VLPs might preclude differentiation between vesicles released constitutively by the cell and those released as a result of viral protein expression.

Inhibition of the ESCRT machinery by a DN mutant of VPS4 negatively influenced the release of VP40-induced filaments. Interestingly, even a mutant of VP40 lacking a functional late domain was dependent on the ESCRT machinery. Since analysis of interactions between VP40 and known ESCRT proteins did not reveal unexpected binding partners, the molecular basis of the interplay between VP40 lacking the late domain and the ESCRT machinery remains enigmatic. Possibly, interaction of VP40 with members of the ESCRT machinery could be facilitated by monoubiquitination of VP40, since many of the ESCRT proteins have ubiquitin-binding properties (33, 61). Interestingly, Urata et al. showed that MARV VP40 is able to interact with Tsg101 in a glutathione *S*-transferase pull-down assay, although the protein does not contain a corresponding late-domain motif (54).

Replacement of the MARV late domain in VP40 with the EBOV VP40 late domain increased the budding of filamentous particles. The EBOV VP40 late domain consists of two overlapping domains, which probably allow the recruitment of more ESCRT proteins to the budding site. Alternatively, different entry points into the ESCRT pathway may have resulted in more efficient budding. The enhancement of budding affected mainly the release of short filaments. The molecular basis for this phenomenon is not understood. Possibly, enhanced recruitment of ESCRT proteins speeds up the process of abscission, resulting in shorter filaments.

In support of the finding that the late domain of VP40 influenced its budding activity, it was demonstrated that a DN mutant of VPS4, which is essential for recycling the ESCRTs (11, 50), inhibited the release of VP40 VLPs into the supernatant. In contrast, the release of vesicles containing cellular proteins did not respond significantly to the expression of DN VPS4. Taken together, these data indicate that while VLPs from the supernatants of VP40-expressing cells are valuable tools for the investigation of the budding of MARV particles, it is important to separate filamentous VLPs from vesicular particles, which contain many cellular proteins and use a different budding mechanism.

MARV VP40 missing the late domain is still sensitive to VPS4 pathway function. The data presented suggested that the interplay of VP40 with the ESCRT machinery is influenced by the known late domain and additionally by other, unknown factors, which make it sensitive to DN VPS4. Yeast two-hybrid screens showed that MARV VP40 interacted with AIP2, AIP4, and AIP5, all Nedd4-like E3 ubiquitin ligases. These interactions are mediated by the known late-domain motif PPxY. The

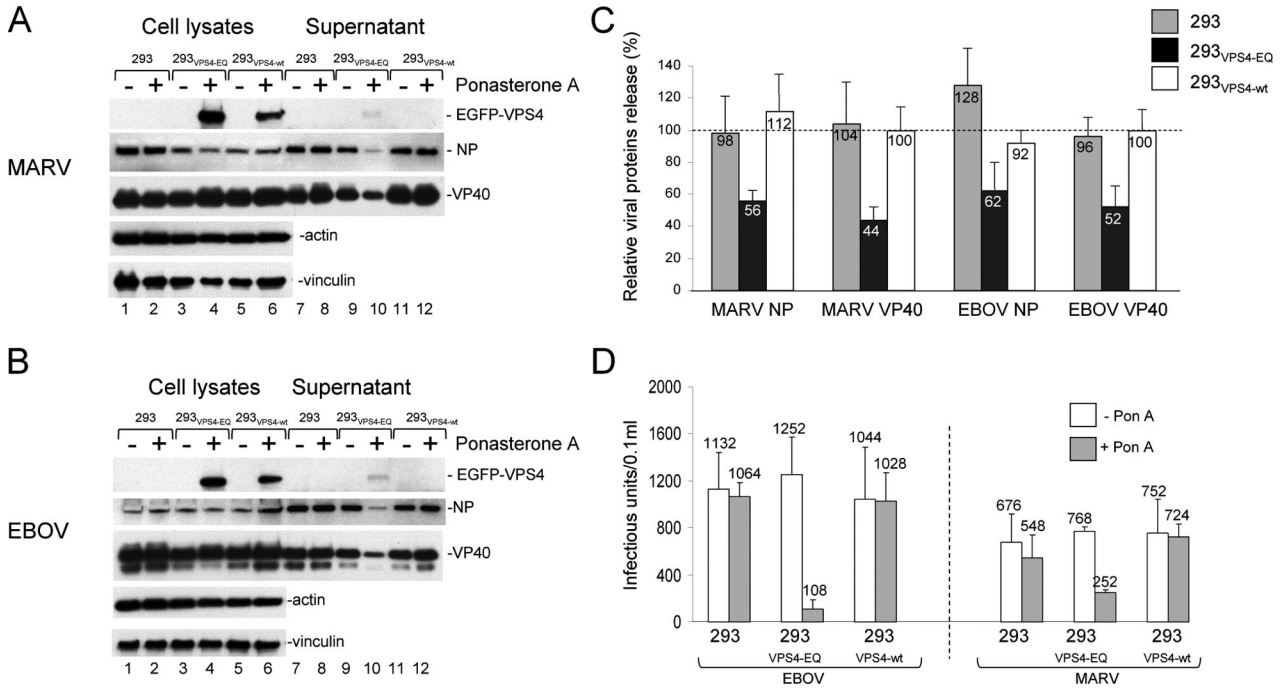

FIG. 6. DN VPS4 inhibits the release of MARV and EBOV proteins. (A and B) HEK 293 or iHEK 293 cells expressing either EGFP-VPS4-wt or EGFP-VPS4-E228Q were infected with either MARV (A) or EBOV (B). Expression of EGFP-VPS4-E228Q and EGFP-VPS4-wt either was not induced or was induced with 1 μM ponasterone A at the time of infection. Cell lysates of filovirus-infected cells and supernatants were collected at 1 day after infection, and Western blot analysis was performed to detect GFP fusion proteins, NP, VP40, and cellular proteins. (C) The intensities of the bands for viral cell- and supernatant-associated NP and VP40 in panels A and B were quantified using the Odyssey imaging system. The relative amounts of released viral proteins in cells that were not treated with ponasterone A were set at 100% (dashed horizontal line). Data are averages and standard deviations from at least three independent experiments. (D) HEK 293 and iHEK 293 cells expressing EGFP-VPS4-wt or EGFP-VPS4-E228Q were infected with either MARV or EBOV. Expression of EGFP-VPS4-E228Q and EGFP-VPS4-wt was either induced (shaded bars) or not (open bars) with 1 μM ponasterone A at the time of infection. Clarified culture supernatants from infected cells were used to infect Vero cells in three sequential dilutions (no dilution, 1:10, and 1:100). Infected Vero cells were fixed and analyzed by an IFF assay 24 h after infection. Graphics show the mean values for infectious MARV and EBOV particles quantified from these three different dilutions.

TABLE 1. Effect of DN VPS4 on filovirus budding

Cell line[a]	$TCID_{50}$[b] (IU/ml) of:	
	EBOV	MARV
HEK 293		
Without ponasterone A	5.2×10^4	9.0×10^3
With ponasterone A	1.6×10^5	9.0×10^3
EGFP-VPS4-E228Q[c]		
Without ponasterone A	3.5×10^5	3.5×10^4
With ponasterone A	9.0×10^3	1.6×10^4
EGFP-VPS4-wt		
Without ponasterone A	9.0×10^4	5.2×10^4
With ponasterone A	9.0×10^4	9.0×10^4

[a] Inducible iHEK293 cell lines (EGFP-VPS4-E228Q and EGFP-VPS4-wt) were incubated without or with ponasterone A to induce the expression of the respective construct. The influence of ponasterone A on filoviral budding in noninducible HEK 293 cells was tested as well.

[b] Cells were infected with EBOV or MARV at a multiplicity of infection of 1.0. Media were collected at 2 days postinfection, and virus titers were determined by a $TCID_{50}$ assay. Viral titers shown represent data from one of three independent experiments.

[c] Viral titers in ponasterone A-induced cells were decreased 17-fold for EBOV and 2.5-fold for MARV from titers in noninduced cells (averages from three independent experiments).

molecular mechanism that inhibited the release of $VP40_{PPxA}$ in the presence of a DN VPS4 remains unclear.

A functional VPS4 pathway contributes to MARV budding but is not essential. The VPS pathway, which is used for the formation of the internal vesicles in MVBs, is a cellular pathway that is hijacked by viruses to enable their pinching off from host cell membranes. Inhibition of the VPS pathway diminished the release of many viruses, and the magnitude of inhibition was remarkably different for different viruses (reviewed in references 5 and 14). While DN VPS4 reduced the budding of retrovirus particles as much as 100- to 1,000-fold (16, 58), minor effects were observed on the budding of EBOV, which was decreased 10-fold (34). For the budding of vesicular stomatitis virus, conflicting results have been published. Irie et al. observed no decrease in the budding of vesicular stomatitis virus in the presence of a DN VPS4, while Taylor et al. detected a 28-fold-diminished budding activity (27, 50). In no instance was a functional VPS pathway essential for budding, which strongly suggests that alternative mechanisms might exist that are used by viruses to enable their release from the infected cell. The variable effects of the VPS pathway on viral budding might be the result of different experimental approaches, i.e., mutation of late-domain motifs, knockdown of ESCRT proteins by small

interfering RNA, or expression of DN mutants of VPS4. Alternatively, these findings may indicate different sensitivities of the different viruses to inhibition of the VPS pathway, as was shown for EBOV and MARV in the present study. For EBOV the finding that budding activity is diminished 10-fold has been published (34), and this result was confirmed in the present study. We also compared the sensitivities of EBOV and MARV budding to the VPS pathway and found that MARV was less sensitive, indicating that even the two filoviruses differ in their degrees of dependence on a functional VPS4 pathway. It is presently unclear whether the VPS pathway plays a significant role in the MARV life cycle and whether the slight diminishment in the release of MARV particles upon expression of DN VPS4 was induced directly by inhibition of budding or by other effects, since overexpression of DN VPS4 also impairs intracellular protein and cholesterol trafficking (6, 15, 45). For the alphavirus Semliki Forest virus, a two- to threefold decrease in budding activity was not considered significant (50). However, the speed of replication of Semliki Forest virus, which produces 1.2×10^9 PFU/ml within 6 h postinfection, is much higher than that of MARV, which produced 5.2×10^3 IU/ml within 24 h postinfection. Since the orchestration of viral replication and the response of the immune system are especially critical in hemorrhagic fever-inducing viruses, whose pathogenesis is influenced in large part by the unsynchronized response of the immune system, even small changes in budding efficiency might have detrimental effects on the outcome of disease. Based on these data, we think that the VPS pathway is one of the mechanisms (some of which remain to be determined) that together drive the budding of MARV.

Taken together, our study established that the release of filamentous VLPs but not vesicular particles from cells expressing MARV VP40 can be considered VP40 driven and can be used as a tool to investigate MARV budding. Induction of filamentous VLPs by VP40 largely excluded incorporation of cellular proteins. Using filamentous VLPs as a model, we then showed that the VPS pathway contributes to VLP release, which is partly mediated by the late-domain motif of VP40. Finally, these results were confirmed by analyzing the release of infectious MARV, which was also partly dependent on the VPS pathway and was on the same order of magnitude as that observed for filamentous VLPs.

ACKNOWLEDGMENTS

We thank Angelika Lander and Ulla Thiesen for expert technical assistance, Sandra Bamberg for providing plasmid pCAGGS-VP40$_{PPxA}$, and Milton Medina for providing plasmid pCAGGS-VP40$_{ELD}$. We are very grateful for the help of Wesley Sundquist, who read and critically discussed the manuscript. We gratefully acknowledge the editing of the manuscript by Allison Groseth.

This work was supported by the Deutsche Forschungsgemeinschaft through SFB 535 TP A1 and by the Schwerpunktprogramm SPP 1175/BE 1325/5-1.

REFERENCES

1. **Babst, M.** 2005. A protein's final ESCRT. Traffic **6:**2–9.
2. **Babst, M., T. K. Sato, L. M. Banta, and S. D. Emr.** 1997. Endosomal transport function in yeast requires a novel AAA-type ATPase, Vps4p. EMBO J. **16:**1820–1831.
3. **Babst, M., B. Wendland, E. J. Estepa, and S. D. Emr.** 1998. The Vps4p AAA ATPase regulates membrane association of a Vps protein complex required for normal endosome function. EMBO J. **17:**2982–2993.
4. **Bess, J. W., Jr., R. J. Gorelick, W. J. Bosche, L. E. Henderson, and L. O. Arthur.** 1997. Microvesicles are a source of contaminating cellular proteins found in purified HIV-1 preparations. Virology **230:**134–144.
5. **Bieniasz, P. D.** 2006. Late budding domains and host proteins in enveloped virus release. Virology **344:**55–63.
6. **Bishop, N., and P. Woodman.** 2000. ATPase-defective mammalian VPS4 localizes to aberrant endosomes and impairs cholesterol trafficking. Mol. Biol. Cell **11:**227–239.
7. **Bishop, N., and P. Woodman.** 2001. TSG101/mammalian VPS23 and mammalian VPS28 interact directly and are recruited to VPS4-induced endosomes. J. Biol. Chem. **276:**11735–11742.
8. **Chen, B. J., and R. A. Lamb.** 2008. Mechanisms for enveloped virus budding: can some viruses do without an ESCRT? Virology **372:**221–232.
9. **Chen, H. I., and M. Sudol.** 1995. The WW domain of Yes-associated protein binds a proline-rich ligand that differs from the consensus established for Src homology 3-binding modules. Proc. Natl. Acad. Sci. USA **92:**7819–7823.
10. **Coronel, E. C., K. G. Murti, T. Takimoto, and A. Portner.** 1999. Human parainfluenza virus type 1 matrix and nucleoprotein genes transiently expressed in mammalian cells induce the release of virus-like particles containing nucleocapsid-like structures. J. Virol. **73:**7035–7038.
11. **Crump, C. M., C. Yates, and T. Minson.** 2007. Herpes simplex virus type 1 cytoplasmic envelopment requires functional Vps4. J. Virol. **81:**7380–7387.
12. **Février, B., and G. Raposo.** 2004. Exosomes: endosomal-derived vesicles shipping extracellular messages. Curr. Opin. Cell Biol. **16:**415–421.
13. **Fraile-Ramos, A., A. Pelchen-Matthews, C. Risco, M. T. Rejas, V. C. Emery, A. F. Hassan-Walker, M. Esteban, and M. Marsh.** 2007. The ESCRT machinery is not required for human cytomegalovirus envelopment. Cell. Microbiol. **9:**2955–2967.
14. **Freed, E. O.** 2002. Viral late domains. J. Virol. **76:**4679–4687.
15. **Fujita, H., M. Yamanaka, K. Imamura, Y. Tanaka, A. Nara, T. Yoshimori, S. Yokota, and M. Himeno.** 2003. A dominant negative form of the AAA ATPase SKD1/VPS4 impairs membrane trafficking out of endosomal/lysosomal compartments: class E vps phenotype in mammalian cells. J. Cell Sci. **116:**401–414.
16. **Garrus, J. E., U. K. von Schwedler, O. W. Pornillos, S. G. Morham, K. H. Zavitz, H. E. Wang, D. A. Wettstein, K. M. Stray, M. Cote, R. L. Rich, D. G. Myszka, and W. I. Sundquist.** 2001. Tsg101 and the vacuolar protein sorting pathway are essential for HIV-1 budding. Cell **107:**55–65.
17. **Gluschankof, P., I. Mondor, H. R. Gelderblom, and Q. J. Sattentau.** 1997. Cell membrane vesicles are a major contaminant of gradient-enriched human immunodeficiency virus type-1 preparations. Virology **230:**125–133.
18. **Gómez-Puertas, P., C. Albo, E. Perez-Pastrana, A. Vivo, and A. Portela.** 2000. Influenza virus matrix protein is the major driving force in virus budding. J. Virol. **74:**11538–11547.
19. **Göttlinger, H. G., T. Dorfman, J. G. Sodroski, and W. A. Haseltine.** 1991. Effect of mutations affecting the p6 gag protein on human immunodeficiency virus particle release. Proc. Natl. Acad. Sci. USA **88:**3195–3199.
20. **Gruenberg, J., and H. Stenmark.** 2004. The biogenesis of multivesicular endosomes. Nat. Rev. Mol. Cell Biol. **5:**317–323.
21. **Harrisson, F., C. Vanroelen, and L. Vakaet.** 1988. Morphological and immunocytochemical studies of fibronectin-coated, plasma membrane-limited vesicles in the early chicken embryo. Anat. Rec. **221:**854–859.
22. **Harty, R. N., M. E. Brown, G. Wang, J. Huibregtse, and F. P. Hayes.** 2000. A PPxY motif within the VP40 protein of Ebola virus interacts physically and functionally with a ubiquitin ligase: implications for filovirus budding. Proc. Natl. Acad. Sci. USA **97:**13871–13876.
23. **Hierholzer, J. C., and R. A. Killington.** 1996. Virus isolation and quantitation. Academic Press Limited, London, United Kingdom.
24. **Hoenen, T., L. Kolesnikova, and S. Becker.** 2007. Recent advances in filovirus- and arenavirus-like particles. Future Virol. **2:**193.
25. **Huang, M., J. M. Orenstein, M. A. Martin, and E. O. Freed.** 1995. p6^{Gag} is required for particle production from full-length human immunodeficiency virus type 1 molecular clones expressing protease. J. Virol. **69:**6810–6818.
26. **Hurley, J. H., and S. D. Emr.** 2006. The ESCRT complexes: structure and mechanism of a membrane-trafficking network. Annu. Rev. Biophys. Biomol. Struct. **35:**277–298.
27. **Irie, T., J. M. Licata, J. P. McGettigan, M. J. Schnell, and R. N. Harty.** 2004. Budding of PPxY-containing rhabdoviruses is not dependent on host proteins TGS101 and VPS4A. J. Virol. **78:**2657–2665.
28. **Justice, P. A., W. Sun, Y. Li, Z. Ye, P. R. Grigera, and R. R. Wagner.** 1995. Membrane vesiculation function and exocytosis of wild-type and mutant matrix proteins of vesicular stomatitis virus. J. Virol. **69:**3156–3160.
29. **Karacostas, V., K. Nagashima, M. A. Gonda, and B. Moss.** 1989. Human immunodeficiency virus-like particles produced by a vaccinia virus expression vector. Proc. Natl. Acad. Sci. USA **86:**8964–8967.
30. **Kolesnikova, L., B. Berghofer, S. Bamberg, and S. Becker.** 2004. Multivesicular bodies as a platform for formation of the Marburg virus envelope. J. Virol. **78:**12277–12287.
31. **Kolesnikova, L., A. B. Bohil, R. E. Cheney, and S. Becker.** 2007. Budding of Marburg virus is associated with filopodia. Cell. Microbiol. **9:**939–951.
32. **Kolesnikova, L., H. Bugany, H. D. Klenk, and S. Becker.** 2002. VP40, the

matrix protein of Marburg virus, is associated with membranes of the late endosomal compartment. J. Virol. **76:**1825–1838.
33. **Langelier, C., U. K. von Schwedler, R. D. Fisher, I. De Domenico, P. L. White, C. P. Hill, J. Kaplan, D. Ward, and W. I. Sundquist.** 2006. Human ESCRT-II complex and its role in human immunodeficiency virus type 1 release. J. Virol. **80:**9465–9480.
34. **Licata, J. M., M. Simpson-Holley, N. T. Wright, Z. Han, J. Paragas, and R. N. Harty.** 2003. Overlapping motifs (PTAP and PPEY) within the Ebola virus VP40 protein function independently as late budding domains: involvement of host proteins TSG101 and VPS-4. J. Virol. **77:**1812–1819.
35. **Martin-Serrano, J., A. Yarovoy, D. Perez-Caballero, and P. D. Bieniasz.** 2003. Divergent retroviral late-budding domains recruit vacuolar protein sorting factors by using alternative adaptor proteins. Proc. Natl. Acad. Sci. USA **100:**12414–12419.
36. **Martin-Serrano, J., T. Zang, and P. D. Bieniasz.** 2001. HIV-1 and Ebola virus encode small peptide motifs that recruit Tsg101 to sites of particle assembly to facilitate egress. Nat. Med. **7:**1313–1319.
37. **Martin-Serrano, J., T. Zang, and P. D. Bieniasz.** 2003. Role of ESCRT-I in retroviral budding. J. Virol. **77:**4794–4804.
38. **Medina, G., Y. Zhang, Y. Tang, E. Gottwein, M. L. Vana, F. Bouamr, J. Leis, and C. A. Carter.** 2005. The functionally exchangeable L domains in RSV and HIV-1 Gag direct particle release through pathways linked by Tsg101. Traffic **6:**880–894.
39. **Mittler, E., L. Kolesnikova, T. Strecker, W. Garten, and S. Becker.** 2007. Role of the transmembrane domain of Marburg virus surface protein GP in assembly of the viral envelope. J. Virol. **81:**3942–3948.
40. **Möller, P., N. Pariente, H. D. Klenk, and S. Becker.** 2005. Homo-oligomerization of Marburg virus VP35 is essential for its function in replication and transcription. J. Virol. **79:**14876–14886.
41. **Nayak, D. P., E. K. Hui, and S. Barman.** 2004. Assembly and budding of influenza virus. Virus Res. **106:**147–165.
42. **Perez, M., R. C. Craven, and J. C. de la Torre.** 2003. The small RING finger protein Z drives arenavirus budding: implications for antiviral strategies. Proc. Natl. Acad. Sci. USA **100:**12978–12983.
43. **Piccin, A., W. G. Murphy, and O. P. Smith.** 2007. Circulating microparticles: pathophysiology and clinical implications. Blood Rev. **21:**157–171.
44. **Pushko, P., T. M. Tumpey, N. Van Hoeven, J. A. Belser, R. Robinson, M. Nathan, G. Smith, D. C. Wright, and R. A. Bright.** 2007. Evaluation of influenza virus-like particles and Novasome adjuvant as candidate vaccine for avian influenza. Vaccine **25:**4283–4290.
45. **Scheuring, S., R. A. Rohricht, B. Schoning-Burkhardt, A. Beyer, S. Muller, H. F. Abts, and K. Kohrer.** 2001. Mammalian cells express two VPS4 proteins both of which are involved in intracellular protein trafficking. J. Mol. Biol. **312:**469–480.
46. **Schmitt, A. P., G. P. Leser, E. Morita, W. I. Sundquist, and R. A. Lamb.** 2005. Evidence for a new viral late-domain core sequence, FPIV, necessary for budding of a paramyxovirus. J. Virol. **79:**2988–2997.
47. **Strack, B., A. Calistri, S. Craig, E. Popova, and H. G. Gottlinger.** 2003. AIP1/ALIX is a binding partner for HIV-1 p6 and EIAV p9 functioning in virus budding. Cell **114:**689–699.
48. **Strecker, T., R. Eichler, J. Meulen, W. Weissenhorn, H. Dieter Klenk, W. Garten, and O. Lenz.** 2003. Lassa virus Z protein is a matrix protein and sufficient for the release of virus-like particles. J. Virol. **77:**10700–10705. (Corrected.)
49. **Swenson, D. L., K. L. Warfield, K. Kuehl, T. Larsen, M. C. Hevey, A. Schmaljohn, S. Bavari, and M. J. Aman.** 2004. Generation of Marburg virus-like particles by co-expression of glycoprotein and matrix protein. FEMS Immunol. Med. Microbiol. **40:**27–31.
50. **Taylor, G. M., P. I. Hanson, and M. Kielian.** 2007. Ubiquitin depletion and dominant-negative VPS4 inhibit rhabdovirus budding without affecting alphavirus budding. J. Virol. **81:**13631–13639.
51. **Théry, C., L. Zitvogel, and S. Amigorena.** 2002. Exosomes: composition, biogenesis and function. Nat. Rev. Immunol. **2:**569–579.
52. **Timmins, J., S. Scianimanico, G. Schoehn, and W. Weissenhorn.** 2001. Vesicular release of Ebola virus matrix protein VP40. Virology **283:**1–6.
53. **Trubey, C. M., E. Chertova, L. V. Coren, J. M. Hilburn, C. V. Hixson, K. Nagashima, J. D. Lifson, and D. E. Ott.** 2003. Quantitation of HLA class II protein incorporated into human immunodeficiency type 1 virions purified by anti-CD45 immunoaffinity depletion of microvesicles. J. Virol. **77:**12699–12709.
54. **Urata, S., T. Noda, Y. Kawaoka, S. Morikawa, H. Yokosawa, and J. Yasuda.** 2007. Interaction of Tsg101 with Marburg virus VP40 depends on the PPPY motif, but not the PT/SAP motif as in the case of Ebola virus, and Tsg101 plays a critical role in the budding of Marburg virus-like particles induced by VP40, NP, and GP. J. Virol. **81:**4895–4899.
55. **Urata, S., T. Noda, Y. Kawaoka, H. Yokosawa, and J. Yasuda.** 2006. Cellular factors required for Lassa virus budding. J. Virol. **80:**4191–4195.
56. **van Niel, G., I. Porto-Carreiro, S. Simoes, and G. Raposo.** 2006. Exosomes: a common pathway for a specialized function. J. Biochem. (Tokyo) **140:**13–21.
57. **VerPlank, L., F. Bouamr, T. J. LaGrassa, B. Agresta, A. Kikonyogo, J. Leis, and C. A. Carter.** 2001. Tsg101, a homologue of ubiquitin-conjugating (E2) enzymes, binds the L domain in HIV type 1 $Pr55^{Gag}$. Proc. Natl. Acad. Sci. USA **98:**7724–7729.
58. **von Schwedler, U. K., M. Stuchell, B. Muller, D. M. Ward, H. Y. Chung, E. Morita, H. E. Wang, T. Davis, G. P. He, D. M. Cimbora, A. Scott, H. G. Krausslich, J. Kaplan, S. G. Morham, and W. I. Sundquist.** 2003. The protein network of HIV budding. Cell **114:**701–713.
59. **Warfield, K. L., D. L. Swenson, G. Demmin, and S. Bavari.** 2005. Filovirus-like particles as vaccines and discovery tools. Expert Rev. Vaccines **4:**429–440.
60. **Welsch, S., B. Muller, and H. G. Krausslich.** 2007. More than one door: budding of enveloped viruses through cellular membranes. FEBS Lett. **581:**2089–2097.
61. **Williams, R. L., and S. Urbe.** 2007. The emerging shape of the ESCRT machinery. Nat. Rev. Mol. Cell Biol. **8:**355–368.
62. **Wills, J. W., and R. C. Craven.** 1991. Form, function, and use of retroviral gag proteins. AIDS **5:**639–654.
63. **Yang, C., L. Ye, and R. W. Compans.** 2008. Protection against filovirus infection: virus-like particle vaccines. Expert Rev. Vaccines **7:**333–344.